Research Article

Bartłomiej Szypuła*

Quality assessment of DEM derived from topographic maps for geomorphometric purposes

https://doi.org/10.1515/geo-2019-0066
Received May 08, 2019; accepted Sep 10, 2019

Abstract: Digital elevation models (DEMs) play a significant role in geomorphological research. For geomorphologists reconstructing landform and drainage structure is frequently as important as elevation accuracy. Consequently, large-scale topographic maps (with contours, height points and watercourses) constitute excellent material for creating models (here called Topo-DEM) in fine resolution. The purpose of the conducted analyses was to assess the quality of Topo-DEM against freely-available global DEMs and then to compare it with a reference model derived from laser scanning (LiDAR-DEM). The analysis also involved derivative maps of geomorphometric parameters (local relief, slope, curvature, aspect) generated on the basis of Topo-DEM and LiDAR-DEM. Moreover, comparative classification of landforms was carried out. It was indicated that Topo-DEM is characterised by good elevation accuracy (RMSE <2 m) and reflects the topography of the analyzed area surprisingly well. Additionally, statistical and percentage metrics confirm that it is possible to generate a DEM with very good quality parameters on the basis of a large-scale topographic map (1:10,000): elevation differences between Topo-DEM and: 1) topographic map amounted from –1.68 to +2.06 m, MAE is 0.10 m, RMSE 0.16 m; 2) LiDAR-DEM (MAE 1.13 m, RMSE 1.69 m, SD 1.83 m); 3) GPS RTK measurements amounted from –3.6 to +3.01 m, MAE is 0.72 m, RMSE 0.97 m, SD 0.97 m. For an area of several dozen km^2 Topo-DEM with 10×10 m resolution proved more efficient than detailed (1×1 m) LiDAR-DEM.

Keywords: DEM, LiDAR, quality assessment, geomorphometry, ArcGIS, Silesian Upland

***Corresponding Author: Bartłomiej Szypuła:** University of Silesia in Katowice, Faculty of Natural Sciences, Institute of Earth Sciences, ul. Będzińska 60, 41-200 Sosnowiec, Poland;
Email: bartlomiej.szypula@us.edu.pl; Tel.: +48 604708406;
Fax: +48 322915865

1 Introduction

Nowadays digital elevation models (DEMs) are commonly used in earth sciences (and more), mainly in geomorphological research [1, 2], landform classifications [3–6], geomorphometry [7–9] or ecological modelling [10] and play a central role in environmental modelling across a range of spatial scales. This versatility of applications probably is due to the increasing availability of free data sources on the Internet on the one hand, and a growing number of free GIS software applications (*i.e.*, GRASS GIS, SAGA GIS, QGIS) on the other one.

There are currently many global and freely-available DEMs (*i.e.*, GLOBE DEM, SRTM, GTOPO 30, ASTER GDEM, AW3D30, DTED-2, EU-DEM). They have dfferent resolutions (from 25x25 m to 1x1 km) and vertical accuracies (from 5-7 m to 300 m). Despite the global coverage and uniformity of the study they do not provide information on bare-earth elevation as they measure elevation of the highest objects above the ground (*i.e.* SRTM3 DEM was generated by C-band radar interferometry, ASTER was developed by collecting in-track stereo using nadir and aft-looking near infrared cameras, AW3D30 was generated by the panchromatic remote-sensing instrument for stereo mapping, etc.). This situation limits the use of global DEMs in geomorphological modelling, especially in large-scale local-regional studies. Of course, in the absence of other sources of information about the height of a given area, they remain the only source of such kind of data. This multitude of available DEMs calls for their verification. It is necessary to remember that working with digital data requires paying particular attention to their quality. The quality of the DEMs is essential for assessing their suitability and determines the quality of the geomorphometric analysis [11–15]. Small errors in DEMs can produce large errors in derived terrain attributes [16], especially second-order derivatives such as curvature [17, 18]. DEM accuracy depends on the type of topography (relief) and ruggedness of the terrain as well as the type of vegetation [19], methods for collecting elevation data, method for DEM generation, type of DEM grid, and DEM resolution [20–22]. The issue of error analysis in DEMs is still current and brought up in litera-

ture [23–27]. Different authors take up this subject for analysis effects of DEM resolution on derived stream network positions [28], assessment of drainage network extractions in a lowrelief area [29], evaluation of DEMs for analyzing drainage morphometric parameters in a mountainous terrain [30], validation and comparison DEMs with geomorphic metrics [31] or DEM usefulness for analyzing fluvial landscape development in mountainous terrains [32].

It was decided to focus my study on the usefulness of DEM for geomorphometric studies, where distinguishing feature (except elevation accuracy) is a primary requirement for information about terrain shape and drainage structure. For this reason elevation contours and streamlines have remained popular sources of primary topographic data. They can be used to construct fine scale digital elevation models by gridding methods that are locally adaptive to surface shape [see 33]. A topographic map at 1:10,000 scale, despite the generalization of reality, is accurate reflection of the topography and, especially, the relief of the terrain. Although contour lines have been used in geography for over 400 years[1], because of their simplicity and comprehensibility they still remain the most common method for storage and presentation of elevation information. Unfortunately, this method is also the most difficult to be properly utilized with general interpolation techniques. The disadvantage lies in the undersampling of information between contours, especially in areas of low relief.

The main goal of this study was to carry out investigations into the quality assessment of DEM derived from topographic maps data (herein called Topo-DEM) for geomorphometric purposes. These analyses consisted of the presentation of freely-available DEMs and checking their vertical accuracy. Proper quality assessment took place through comparing the accuracy of Topo-DEM with reference to DEM derived from laser scanning (LiDAR-DEM). To achieve this goal it was decided to answer the questions: What is the vertical accuracy of DEM based on digitized topographic maps (1:10,000) and freely-available DEMs: ASTER GDEM, AW3D30, DTED-2, EU-DEM and SRTM like? And can a DEM based on digitized topographic maps (1:10,000) produce similar results for geomorphometric analyses to LiDAR data derived DEM? To answer these questions comparison of elevation differences between a Topo-DEM and a LiDAR-DEM were done, calculations of basic geomorphometric parameters and landform classification using Topographic Position Index were conducted.

1 The concept of the elevation contour to describe topography dates to 1584 when the Dutch surveyor Pieter Bruinz drew lines of equal depth in the River Spaarne; but this was an unpublished manuscript [34].

2 Study area

The study area is located in southern Poland, in the Silesian-Cracow Upland, which belongs to the strip of Polish Uplands [35]. The midpoint of the research area is situated at 50.3° N latitude and at 19.1° E longitude. This area covers over 82 km^2 (Figure 1). When we look at geology, we will see that the highest parts of this area are built of resistant rocks Lower- and Middle-Triassic (mainly limestones and dolomites) and Carboniferous Pennsylvanian Lower (gray shales and sandstones). Lower places and depressions are covered with Pleistocene deposits of glacial sands, gravels and clays [36, 37]. Regarding land cover, it has mainly an anthropogenic character: the largest area occupy anthropogenic, artificial surfaces (urban fabric 38%, industrial, commercial and transport units 12%, green urban areas 7% and mine, dump and construction sites 1%); second group are agricultural areas (arable land 31%) and the third group are forests (ca. 10%). The geomorphological background is made up of two big plateaus separated by a floodplain in the southern part. The northern part of the area consists of river terraces and there are residual hills (due to rock hardness) in the north-west. Moreover, there are many anthropogenic landforms, especially in the centre and south of the area. Anthropogenic flats, subsidence basins and embankments and flood embankments occur near artificial river channels [38]. Local relief is 136 m and the average altitude is 277 m a.s.l. The highest elevations, *i.e.*, St. Dorothy Hill (381 m a.s.l.) and Parcina Hill (355 m a.s.l.) are located in the NW part of the area and the lowest place - an old coal mine area (238 m a.s.l.) in the SW part. The main drainage river is Przemsza with its tributaries and fragment of Brynica with its tributary Wielonka (Figure 1). This area is diverse enough to show different types of landforms but, at the same time, it has well-recognized topography, which constitutes the reason for its selection.

3 Data

3.1 Digital elevation models

The following DEMs were used in this research: LiDAR-DEM, DTED-2, SRTM, ASTER GDEM, AW3D30 and EU-DEM (Table 1 and Figure 2).

LiDAR-DEM [39] Light Detection and Ranging DEM is a digital elevation model derived by Airbone Laser Scanning (ALS) with 1x1 m horizontal resolution and vertical accuracy of 0.2 m [40]. All elevation data are using the PUWG-

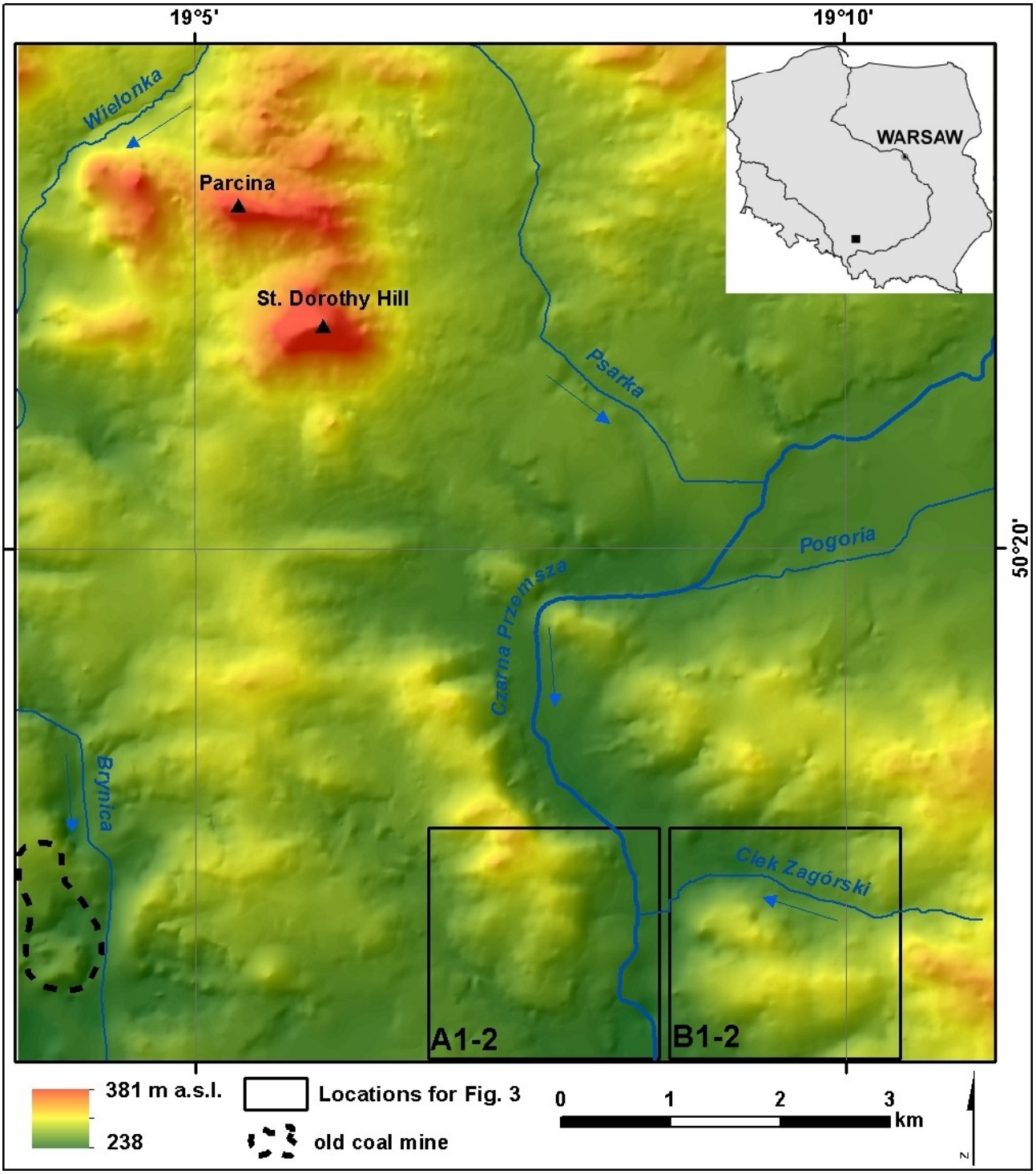

Figure 1: Study area location and hypsometry (on the basis Topo-DEM)

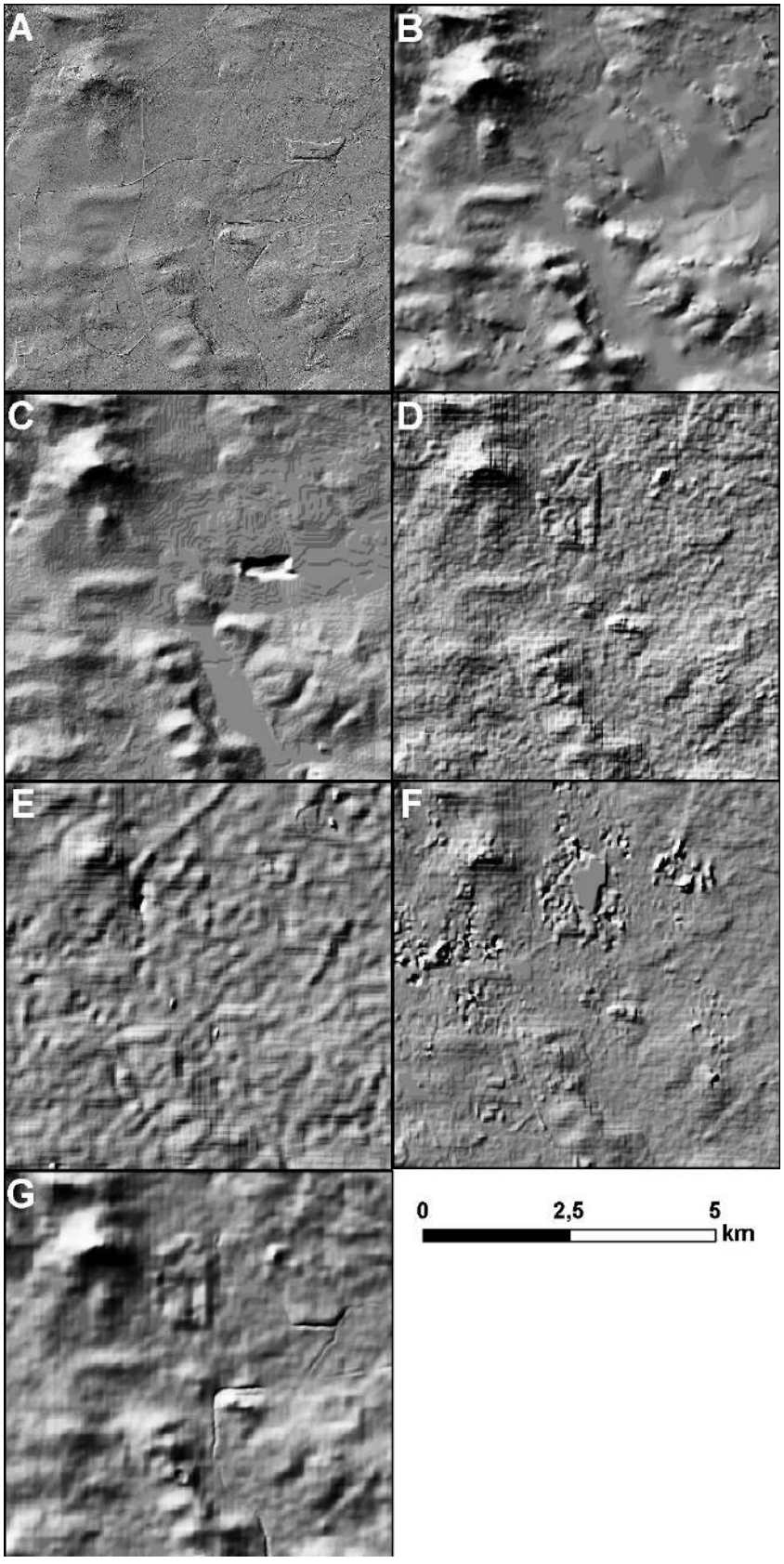

Figure 2: Hillshaded maps: LiDAR-DEM (A), Topo-DEM (B), DTED-2 (C), SRTM (D), ASTER GDEM (E), AW3D30 (F), EU-DEM (G)

Table 1: Basic parameters of used DEMs

DEM Name	Resolution (cell size) [m]	Elevation [m] Min	Max	Mean	SD	Official accuracy (vertical/ horizontal)	Years of data acquisition	Institution, Year of release
LiDAR-DEM	1.0 × 1.0	238.4	381.5	277.3	16.7	**0.2 m / 0.5 m**	2012-2014	Head Office of Geodesy and Cartography, 2014
Topo-DEM	10.0 × 10.0	244.4	380.8	277.5	16.6	-	-	-
DTED-2	24.8 × 24.8	216.0	379.0	277.3	16.8	**18 m / 23 m**	1998-2001	Military Geodesy and Remote Sensing Centre, 2001
SRTM v.3	24.7 × 24.7	235.0	382.0	276.5	16.6	**10 m / 13 m**	2000	NASA and JPL, 2013
ASTER GDEM	24.7 × 24.7	183.0	364.0	262.0	17.0	**20 m / 30 m**	2001-2008	NASA and METI, 2009-2011
AW3D30 v.1.1	24.7 × 24.7	220.0	390.0	277.5	16.9	**5 m / 5 m**	2006-2011	EORC, JAXA, 2017
EU-DEM v.1.1	25.0 × 25.0	242.0	376.1	278.5	16.4	**7 m / 1-5 m**	2003-2009	EEA, Copernicus, 2016

1992 (EPSG: 2180) coordinate system and the heights of points relate to the Normal Height System Kronsztadt 86. This DEM is in ESRI ASCII Grid (asc) format. The source data used to create this DEM were LAS files. Every LAS dataset file contains an average of 7.5 points/m^2 for the entire area [41]. This format consists of header information containing a set of parameters which can be used to geocode the data. Although the header includes the coordinates of the lower left corner of the area covered by the grid, the elevation data are given as strings of elevations, row by row, starting from the upper left point on the grid.

DTED-2 [42] is Digital Terrain Elevation Data of Poland obtained by digitizing of Military Topographic Maps 1:50,000 [43]. In accordance with guidelines [44] this DEM has spatial resolution of 1" latitude and 1" longitude (for this area is 24.8×24.8 m); the assumed absolute horizontal accuracy is < 23 m and vertical accuracy < 12-18 m. The coordinate system is WGS-84 (EPSG: 4326).

SRTM [45] Shuttle Radar Topography Mission data sets result from a collaborative effort of National Aeronautics and Space Administration (NASA) and National Geospatial-Intelligence Agency (NGA), as well as the participation of German and Italian space agencies. This collaboration aims at generating a near-global digital elevation model (DEM) of the Earth with data points posted every 1 arc-second (approximately 30 m) using radar interferometry [46]. The absolute height error of SRTM data sets is 5–10 m and absolute geolocation error is 7–13 m [47, 48]. Improvements and changes that have been made from previous versions include: Voids in the version 3.0 products have been filled with values from the ASTER GDEM version 2.0 [49], the Global Multi-resolution Terrain Elevation Data 2010 GMTED2010 [50], and the National Elevation Dataset [51].

ASTER GDEM [52] Advanced Spaceborne Thermal Emission and Reflection Radiometer Global Digital Elevation Model is a DEM that was developed jointly by NASA and Japan's Ministry of Economy, Trade and Industry (METI). ASTER is capable of collecting in-track stereo using nadir and aft-looking near infrared cameras. Since 2001 these stereo pairs have been used to produce single-scenes (60×60 km) that cover land surfaces between 83°N and 83°S with estimated accuracies of 20 m at 95% confidence for vertical data and 30m at 95% confidence for horizontal data [53]. This model is distributed as georeferenced tagged image file format (GeoTIFF) files. The data grid has a resolution of 1 arc-second (approximately 30 m) and is referenced to the WGS84/1996 Earth Gravitational Model (EGM96) geoid. Although the ASTER GDEM v. 002 is a better model than ASTER GDEM v. 001, users have to know that the data may still contain anomalies and artefacts. One should know that these mistakes can introduce large elevation errors on local scales [54].

AW3D30 [55] ALOS Global Digital Surface Model "ALOS World 3D - 30m" is a global digital surface model (DSM) at 1 arc-second (approximately 30 m) resolution that was released by the Japan Aerospace Exploration Agency (JAXA). This model has been compiled with images acquired by the advanced land observing satellite (ALOS). The elevation data are published based on the DSM data set (5-m mesh version) of the 'World 3D Topographic Data' [56]. A huge amount of stereo-pairs images derived from satellite mission in the years 2006–2011 were source data. Next, they were processed semi-automatically to provide

a digital surface model (DSM). The horizontal resolution of the dataset is 5×5 m [56] and the height accuracy is approximately <5 m from the evaluation with ground control points (GCPs) or reference DSMs derived from LiDAR in WGS-84 coordinate system [57, 58].

EU-DEM [59] Digital Elevation Model over Europe from the GMES RDA project is a hybrid product based mainly on SRTM and ASTER GDEM but also publicly available Russian topographic maps for regions north of 60°N latitude. The data are fused by a weighted averaging approach and they have been generated as a contiguous dataset divided into 1x1 degree tiles. The spatial reference system is geographic, lat/lon with horizontal datum ETRS89, ellipsoid GRS80 and vertical datum EVRS2000 with geoid EGG08 [60]. EU-DEM v. 1.1. is a resulting dataset of the EU-DEM v1.0 upgrade, which enhances the correction of geopositioning issues, reducing the number of artefacts, improving the vertical accuracy of EU-DEM using ICESat as reference and ensuring consistency with EU-Hydro public beta [61]. EU-DEM v1.1 is available in Geotiff 32 bits format at 25 m resolution with vertical accuracy of 7 m RMSE and horizontal 1 m (lowlands) to 5 m RMSE (mountains) [60].

3.2 Topo-DEM

4 sheets of the topographic maps in 1:10,000 scale were the basic data used to create the DEM [62]. Altogether, most of the contour lines (more than 747 km in total) and all 362 points with described altitude were digitized from the maps (Figure 3). Following the cartographical rule, that one should always compile a map from source materials of the same or larger map scales [63]. In the digital environment one have to create a raster map from data at the same or higher spatial resolution than the ground resolution of my map display grid cells. The ground resolution of the map display grid cells will depend on the scale of the map. Since the scale of the source maps was 10,000 (if the smallest polygonal object on the map is 1×1 mm - in reality it is 10×10 m) it was decided to build a DEM with the resolution of 10×10 m - Topo-DEM. The same as LiDAR-DEM, Topo-DEM was made in PUWG-1992 (EPSG: 2180) coordinate system, and the heights of points relate to the Normal Height System Kronsztadt 86 [64].

Digitalization of contours and height points, building Topo-DEM, all analyses and calculations, and DEM visualizations were performed in the ArcGIS environment [65]. Additionally, visual evaluation of the Topo-DEM was made using ArcScene. Moreover one used the QGIS software to verify the correctness of the contours generated from the Topo-DEM by ArcGIS (see paragraph 5.1 and Figure 4), but the results were identical. One have used the Topo-to-Raster tool from ArcGIS Toolbox to generate Topo-DEM. The Topo-to-Raster tool applies an interpolation method specifically designed to create a surface that more closely represents a natural drainage surface and better preserves both ridgelines and stream networks from input contour data. Therefore, all the watercourses and water reservoirs with an area ≥ 500 m^2 were used as breaklines together with contours and height points to support the interpolation process.

This technique creates hydrologically correct DEMs and is based on the ANUDEM algorithm developed by Hutchinson [66–70]. At the beginning of the interpolation process, Topo-to-Raster uses information inherent in the contours to build an initial generalized drainage model. This is done by identifying the points of local maximum curvature in each contour. A network of curvilinear streams and ridges intersecting these points is then derived using the initial elevation grid [66]. The locations of stream and ridge lines are repeatedly corrected and updated as DEM elevations are repeatedly corrected and updated. This information is used to checking hydrogeomorphic properties and to verify accuracy of the output DEM [71].

4 Methods

The performed analyses related to Topo-DEM quality assessment can be divided into three basic stages: 1) preliminary visual assessment based on topographic maps; 2) the juxtaposition of altitude accuracy and field measurements in relation to other available DEMs; 3) quantitative and statistical comparison of the elevation and geomorphological accuracy with LiDAR-DEM.

The first stage consisted in the observation of the model in a 3D view with a topographic map draped on a DEM. Owing to this, the explicit spatial position of the most important elements of the topography (river valleys, the course of ridges, peaks, etc.) was verified. Then, the course of contours generated from the model was compared with original contours from topographic maps. In the last step, 100 checkpoints were randomly generated for which elevations read from the topographic map and from the Topo-DEM were compared.

The second stage was the analysis of the vertical accuracy all the DEMs. Vertical accuracy is one of the most important features of DEMs used for geomorphometric relief analysis. Sometimes accuracy assessment of a DEM is carried out by means of reference data called ‘checkpoints’ (or

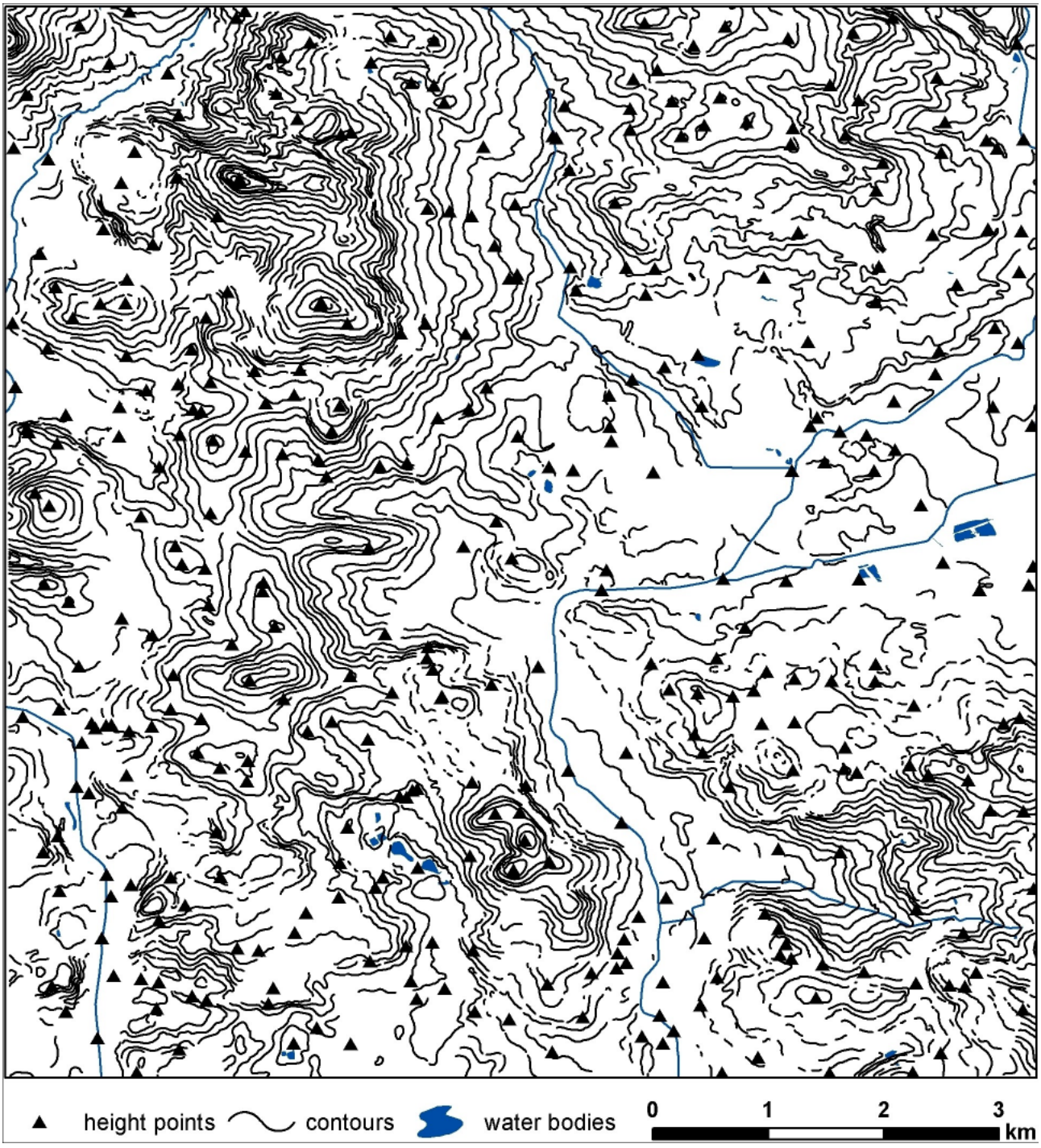

Figure 3: Digitized contour lines, elevation points and water-courses

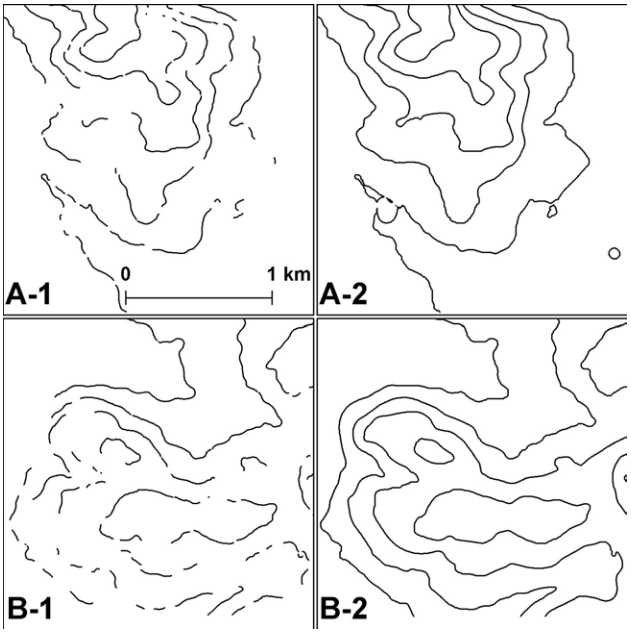

Figure 4: Example of the 10m-contours digitized from the topographic map (A-1, B-1) and derived from the Topo-DEM (A-2, B-2)

'reference points'). DEM accuracy is commonly estimated by the criterion of elevation differences and RMSE of elevation computed by comparing DEM points and checkpoints [23]. Höhle & Höhle [72] pointed out that checkpoints should be: 1) at least three times more accurate than the DEM elevations being evaluated [see also 73] distributed randomly, 3) the number of checkpoints (sample size) should be sufficiently large in order to obtain reliable accuracy measures. The American Society of Photogrammetry and Remote Sensing (ASPRS) recommends a minimum of 20 checkpoints in each of the major landform categories [74]. On the basis of Digital Geomorphological Map of Poland [38] five major landform categories (excluding small landforms related to human activity) for this area were distinguished. They included: planation surfaces (in watershed setting), residual hills (due to rock hardness), plateaus, floodplains and river terraces. In case of these five landform categories a minimum of 100 checkpoints were required.

According to the above assumptions, reference data were derived by ground surveying with the application of high precision GPS RTK Leica Viva CS10. In total, 149 points for the entire area were measured (Figure 6). It is clearly visible that the distribution of checkpoints was not very regular because it was related to specific landform types. The number of checkpoints measured within each landform was over 20 and the average accuracy of all the GPS RTK surveys was 1cm (horizontal) and 1.3 cm (vertical) (Table 2).

Table 2: GPS RTK surveys with reference to landforms

Landforms	Number of checkpoints	Average surveys accuracy [m]	
		horizontal	vertical
planation surface (in watershed setting)	22	0.010	0.013
residual hills (due to the rock hardness)	31		
Plateaus	40		
Floodplains	23		
river terraces	33		

The final stage was a detailed comparative analysis of Topo-DEM with LiDAR-DEM. As said it has been pointed out above, the evaluation of DEM accuracy is usually performed by RMSE and difference height calculation of DEM points and reference points. Obviously, the number of reference points is limited. This can lead to improper estimation of RMSE. This approach was elaborated by Rieger [75], who proposed comparing a target DEM with a "reference" DEM. In this case, LiDAR-DEM was accepted as a reference model because of its source material (ALS cloud points) features: 1) the area being regularly covered with measurement data, 2) high measurement density, *i.e.*, 4 to 12 pts/m^2 [32], average 7.5 pts/m^2 for this area [41], 3) high vertical accuracy (<0.2 m) and 4) small number of noise (erroneous measurements). Therefore, further calculations of errors and derivatives of Topo-DEM were based on comparisons with LiDAR-DEM.

Apart from standard methods of evaluating the absolute accuracy of DEMs, in geomorphometry and geomorphology we are often more interested in land-surface parameters. High-resolution DEMs are not always the best sources for geomorphometric analysis [16]. It is more important that a DEM accurately reflects the actual shapes and flow/deposition processes of the land surface. This resemblance is often referred to as the 'relative' or 'geomorphological' accuracy of DEMs [76–78]. Geomorphological accuracy defines a general situation of the topography of a given area, on the one hand, emphasizing the most important relief features and, on the other hand, faithfully reproducing the nuances and details of the relief, depending on the DEM spatial resolution and the size of the research area. It is geomorphometry uses DEMs to quantitatively describe the earth's surface. This quantification is expressed by many topographic parameters and indices [see 79] which can be derived from DEMs. Herein one chose

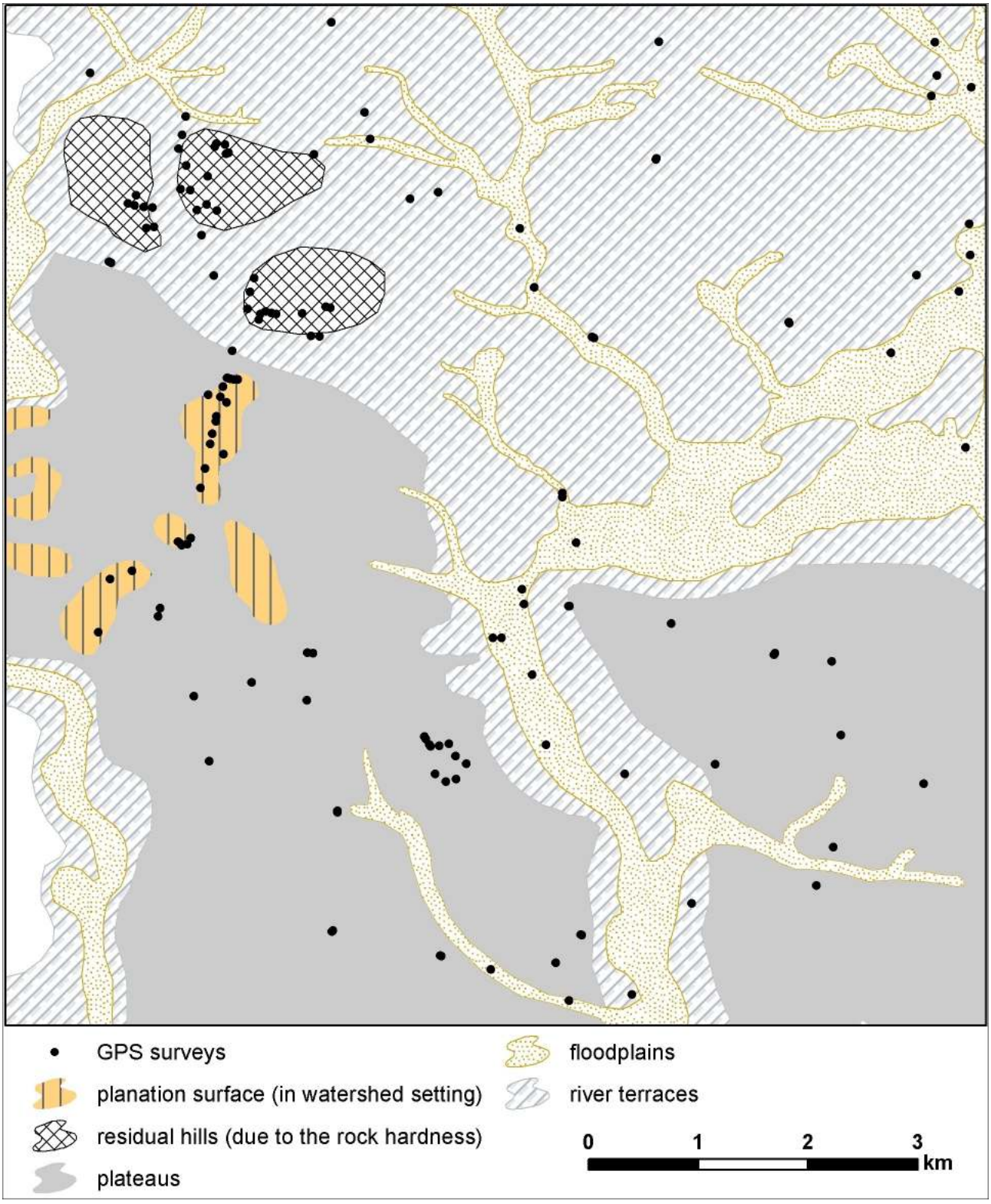

Figure 5: Locations of the GPS surveys in the study area

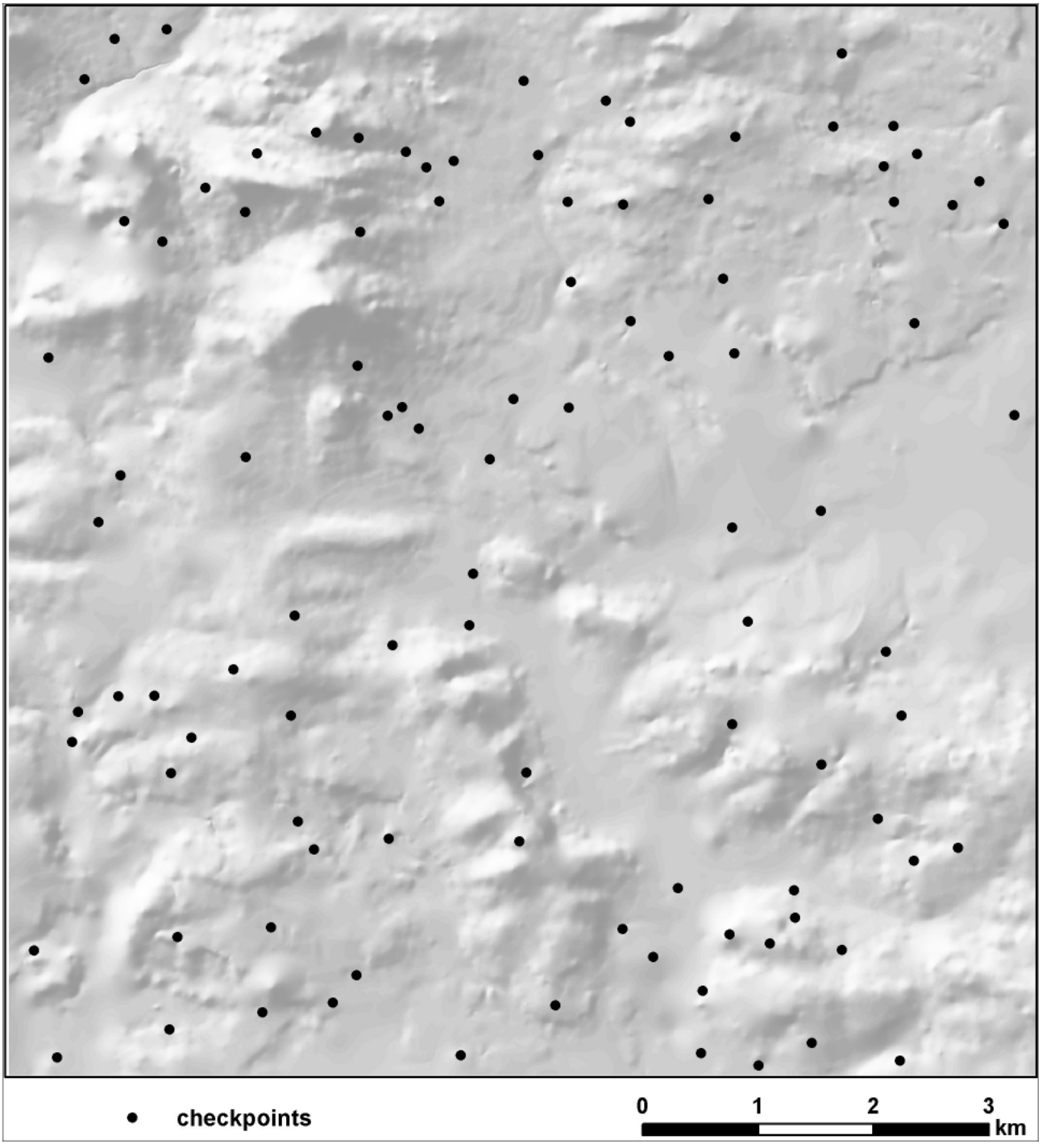

Figure 6: Spatial distribution of the random checkpoints

Table 3: Geomorphometric parameters of DEMs and their statistics

Parameter	Topo-DEM			LiDAR-DEM		
Altitude [m a.s.l.]						
Min		244.4			239.2	
Max		380.8			381.0	
Mean		277.5			277.3	
SD		16.6			16.7	
Local relief [m]	3×3	10×10	25×25	3×3	10×10	25×25
Min	0.0	0.0	0.1	0.0	0.1	0.9
Max	8.9	32.4	63.4	19.1	38.6	64.8
Mean	0.9	3.9	9.8	1.3	5.0	11.3
SD	0.8	3.3	7.2	1.3	3.6	7.2
Slope [°]						
Min		0.0			0.0	
Max		18.5			41.1	
Mean		2.00			2.67	
SD		1.78			2.87	
Curvature [1/100 of m]						
Min		−5.48			−24.01	
Max		3.87			25.40	
Mean		−0.02			−0.10	
SD		0.10			1.28	
Aspect [°]			%			
N (337.5-360.0, 0.0-22.5)		11.0			11.8	
NE (22.5-67.5)		10.5			11.2	
E (67.5-112.5)		12.0			12.3	
SE (112.5-157.5)		13.5			12.9	
S (157.5-202.5)		17.9			17.6	
SW (202.5-247.5)		16.0			14.3	
W (247.5-292.5)		10.2			11.0	
NW (292.5-337.5)		8.8			9.1	

Table 4: Elevation differences between LiDAR-DEM and Topo-DEM

Experiment	Elevation differences between LiDAR-DEM and Topo-DEM[m]				
	Min	Max	MAE	RMSE	SD
version 1	−20.48	22.40	1.13	1.66	1.80
version 2	−20.48	21.77	1.16	1.69	1.83

the most commonly used geomorphometric local parameters (altitude, aspect, slope, curvature) and statistical measures (local relief, standard deviation, etc.) [see 80, 81]. All parameters and their statistics have been presented in Table 3. It should be noted that due to better fit both DEMs, the LiDAR-DEM used to these basic geomorphometric parameters was rescaled (converted) to 10x10 m resolution (see comments to Table 4).

In the last step, the classification of landforms for both models was made, owing to which real assessment of the suitability of Topo-DEM for geomorphometric purposes was possible. Based on previous experience with landform classification [82], it was decided to make calculations using the Topographic Position Index (TPI). TPI has its origins as a landscape position model described by Fels & Zobel [83] and later developed and described in detail by Weiss [84]. Topographic Position Index is fairly simple; it is a classification system based on the difference between a cell elevation value and the average elevation of the neighborhood around that cell. Positive values mean the cell is higher than its surroundings (summit or near the top of a hill or a ridge), while negative values mean it is lower (at or near the bottom of a valley). TPI values near zero could mean either a flat area or a mid-slope area.

When comparing height differences, the following statistical measures were used: Mean Absolute Error (MAE), Root Mean Square Error (RMSE) and Standard Deviation (SD).

MAE, which measures the average magnitude of errors in a set of predictions without considering their direction, is the average of the absolute differences between an actual observation (y_j) and prediction (y_i) at N stations (number of control points used for calculation), where all individual differences have equal weight (Eq. 1).

$$MAE = \frac{\sum_{i-1}^{N} (y_i - y_j)}{N - 1} \tag{1}$$

RMSE, a quadratic scoring rule that also measures the average magnitude of error, is the square root of the average of squared differences between an actual observation (y_j) and prediction (y_i) at N stations (Eq. 2). RMSE is the most frequently used characteristics determining the degree of accuracy or the measure of conformity between a set of estimates and the actual values [85]. It expresses the dispersion of frequency distribution of variances between original (actual) height data and DEM data.

$$RMSE = \sqrt{\frac{\sum_{i-1}^{N} (y_i - y_j)^2}{N - 1}} \tag{2}$$

The MAE and the RMSE can be used together to diagnose the variation in the errors in a set of forecasts. The RMSE will always be larger or equal to the MAE; the greater the difference between them, the greater the variance in the individual errors in the sample. If the RMSE=MAE, then all the errors are of the same magnitude.

Standard deviation (SD) is a statistic measure of the dispersion of a dataset relative to its mean. It is calculated as the square root of variance by determining the variation between each data point (x_i) relative to the mean ($\bar{x}$), and N is the number of observations in the sample (Eq. 3). It is a measure of how spread out numbers are. A low standard deviation indicates that the data points tend to be close to the mean (also called the expected value) of the set, while a high standard deviation indicates that the data points are spread out over a wider range of values [86].

$$SD = \sqrt{\frac{\sum_{i=1}^{N} (x_1 - \bar{x}_2)^2}{N - 1}} \tag{3}$$

5 Results

5.1 Topo-DEM versus source topographic maps

At the beginning, it was decided to make a visual evaluation of a Topo-DEM model. In the ArcGIS software using the ArcScene module [65] this DEM was displayed in a 3D form and rasters of the topographic source maps were draped on it. This procedure made it possible to conduct spatial assessment of the general compatibility of the relief features on a 3D model. It turned out that the created Topo-DEM reflects the general character of the morphology of the study area very well; even some details of the relief related to human activity were visible.

In the next step, all the 10 m contours from the model were generated and compared with the original contours from the topographic maps (Figure 4). The vast majority of the contours generated from the model exactly matched the original course of the contours from topographic maps. It is proof that the method has recreated a DEM with the same characteristics as the original. After calculating the total length of both sets of the contours, it turned out that the contours on the topographic maps have the length of 262 km, while the contours generated from the model measured as many as 329 km, *i.e.* 25% more. This is evidently due to incomplete selection of the course of contour lines on topographic maps (Figure 4A-1, B-1), especially in urban areas (with compact buildings). Such situations (deficiencies in the course of contours) do not appear on the raster model (Figure 4A-2, B-2) as a DEM always represents continuous data. Occasionally there were errors in the contours generated from the model (Figure 4A-2).

In the end 100 checkpoints were randomly generated, for which elevations from the topographic maps were read and compared with the elevations obtained from the Topo-DEM model (Figure 5). The differences in the compared elevations ranged from –1.68 m to +2.06 m. The values of the MAE and RMSE were < 0.2 m, and SD was 0.4 m, which is a very good outcome (Table 5).

The above results allow one to conclude that the DEM with a resolution of 10×10 m derived from topographic

Table 5: Elevation differences between Topo-DEM and a topographic map

Elevation differences [m]				
Min	**Max**	**MAE**	**RMSE**	**SD**
–1.68	2.06	0.19	0.16	0.40

Table 6: Elevation differences between GPS RTK measurements and DEMs values

DEM Name	Resolution (cell size) [m]	Elevation differences [m]					Mean elevation of all checkpoints [m a.s.l.]
		Min	Max	MAE	RMSE	SD	
LiDAR-DEM	1.0 × 1.0	−3.7	+3.4	0.13	0.48	0.48	288.2
Topo-DEM	10.0 × 10.0	−3.6	+3.1	0.72	0.97	0.97	288.3
DTED-2	24.8 × 24.8	−5.5	+6.0	1.26	1.74	1.72	287.9
SRTM v.3	24.7 × 24.7	−11.4	+5.3	2.06	2.68	2.42	287.1
ASTER GDEM	24.7 × 24.7	−6.8	+32.7	16.85	17.3	4.50	271.5
AW3D30 v.1.1	24.7 × 24.7	−22.7	+6.1	2.17	3.13	2.96	287.2
EU-DEM v.1.1	25.0 × 25.0	−10.0	+3.3	1.59	2.18	1.99	289.1
		GPS · RTK					**288.2**

maps corresponds to the precision assumed for this type of study. Borkowski [87] stated that for data obtained from a topographic map at the scale of 1:10,000, the average altitude error is in the range from 0.8 to 2.0 m.

The shift error between LiDAR-DEM and Topo-DEM was not taken into account because: shift error of the LiDAR-DEM is < 0.5 m, mean shift error of the topographic map vs the reference data (high-resolution orthophotomap) is < 2.04 m and contour line width on the topographic map is 1.5-2.0 m. In such case comparison of both DEMs with each other excludes the real calculation of the shift error, because LiDAR-DEM has 100 times higher resolution. The horizontal accuracy that has been achieved within the range of 1 pixel of the Topo-DEM (10×10 m) is sufficient for mapping [see 88]. In conclusion - the shift error is smaller than the Topo-DEM resolution.

5.2 Vertical accuracy of DEMs

Table 6 presents numerical statistics describing height differences between the checkpoints (measured in the field) and the same locations (read from the DEMs). The best results were obtained for LiDAR-DEM. It comes as no surprise, due to the highest sample density and resolution of this DEM. MAE value for this model was only 0.13 m, and RMSE and SD less than 0.5 m. In addition, following careful analysis of the data, it appeared that differences exceeding 0.75 m occur only in 4 points. The mean height of all checkpoints is also exactly the same in LiDAR-DEM as RTK GPS measurements (Table 6).

Among the rest of the models, the best accuracy results were achieved by Topo-DEM: MAE value was only 0.72 m and RMSE and SD less than 1 m. The biggest differences did not exceed 3 m (but only for 2 points out of 149, which is just over 1% of all points). These are amazingly good results, especially in comparison with LiDAR-DEM, which has a hundredfold higher resolution. As for other models, DTED-2 and EU-DEM, which, despite a larger cell size (25×25 m) than Topo-DEM, achieved MAE values of approx. 1.5 m and RMSE and SD from 1.7 to 2.2 m, still deserve attention (Table 6). The worst results were definitely obtained for ASTER GDEM, with maximum errors exceeding 30 m, MAE and SD approx. 17 m. But superficial visual evaluation of this model for the study area shows many artifacts and errors. However, the creators of ASTER GDEM still repeat that this DEM is prone to serious errors, which one should bear in mind [54].

5.3 Topo-DEM versus LiDAR-DEM

5.3.1 Elevation differences

The histograms with elevation distribution of both DEMs are similar and show typical right-skewed (positive) distribution (Figure 7). This situation indicates the prevailing number of altitude values below average elevation values. At the beginning elevation differences between Topo-DEM and LiDAR–DEM were calculated. First calculations were made for LiDAR-DEM in the original (1×1 m) resolution (Table 4 version 1), and then LiDAR-DEM was rescaled (converted) to 10×10 m resolution (version 2). As presented in Table 4, the differences for both resolutions are minimal. The spatial distribution of elevation differences was also almost identical. It can be concluded that the LiDAR-DEM resolution does not have a significant influence on the calculation of elevation differences because the ArcGIS program calculates the result in accordance with the lowest resolution of the input raster (*i.e.*, maximum of input). The accuracies of Topo-DEM are shown in Table 4, where the value −20.48 m represents the negative maximum error and the values 21.7 m and 22.4 m refer to positive maximum errors. However, these extremely high values did not affect

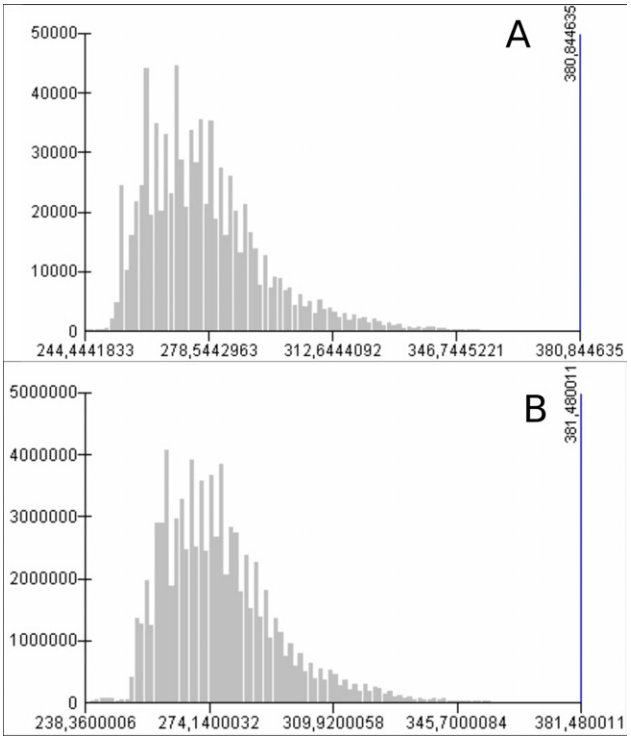

Figure 7: Histograms with elevation distribution of Topo-DEM (A) and LiDAR-DEM (B)

small MAE (1.16 m), RMSE (1.69 m) and SD (1.83 m) because errors bigger than ±10 m are only 0.34% of all compared values.

Unfortunately, the disadvantage of RMSE error calculation is that it is usually only globally reported, so no indication of the error spatial distribution is given [85, 89]. This problem is solved by a differential height map between the analyzed Topo-DEM and LiDAR-DEM. Figure 8 shows spatial distribution of elevational changes between both models. The largest elevation differences occurred in places heavily transformed by man: a sewage treatment plant, a former coal mine or a rubbish dump. These are the areas with the smallest number of height information (the course of the contours was uncertain and often incomplete and there were no height points).

Sharma, Tiwari & Bhadoria [90] noted that results substantiate the finding that the accuracy provided in form of RMSE alone is not sufficient to assess the quality of DEM. Therefore, DEM quality should always be considered in view of its application and purpose. Hence the last analyzed aspect was the result conformity of elevations between DEMs, proposed by Szypuła [41]. This method consists in comparing both DEMs cell-by-cell and calculating the differences between them. Herein, result conformity values express how many percent of the Topo-DEM grid cells are in accordance with the same grid cells of LiDAR-DEM. Conformity was calculated for different elevation ranges: ± 0.1 m, 0.25 m, 0.5 m, 1.0 m and 2.0 m (Table 7). It is interesting that more than 63% of the study area has result conformity value for the height difference of ± 1m and for more than 86% of the area it is ± 2 m. Obviously, the greater the elevation range, the higher result conformity. It generally shows how accurate Topo-DEM is.

Table 7: Result conformity of elevation between LiDAR-DEM and Topo-DEM

Range of elevational differences [m]	Percentage [%]
−0.10 - 0.10	7.9
−0.25 - 0.25	19.6
−0.50 - 0.50	37.4
−1.00 - 1.00	63.4
−2.00 - 2.00	86.1

5.3.2 Basic geomorphometric parameters

Table 3 presents used geomorphometric parameters and their statistics. The first of these was altitude. It is understood as vertical distance from the reference level-surface with the height of 0 (the mean sea level) and expressed in meters above sea level. The Figure 9 shows that, despite the same resolution (10×10 m), LiDAR-DEM is much more detailed. This concerns elements related to human activity (embankments and road-rail incisions, excavations and dumps, artificial river channels, anthropogenic flats) in particular. It is obviously impossible to present all these landforms on a topographic map at the scale of 1:10,000 with great detail. Only the minimum values differ in five meters between the DEMs, this mainly concerns the SW fragment of the area where anthropogenic landforms are located. Maximum, mean and SD values of the altitude are practically the same (Table 3).

The next feature was local relief, which is altitude range between the highest and the lowest points expressed in meters. Calculations were made in filter windows (3×3, 10×10 and 25×25 cells) to check how the values are distributed. Results in Table 3 show that the biggest differences between the models occur for the 3×3 cells neighborhood. This situation confirms much greater detail of LiDAR-DEM compared to Topo-DEM. The larger the filtering window (neighborhood) is, the more convergent and similar the results are. This agrees with the conclusions of Raaflaub & Collins [91], who evaluated the effects of DEM errors on the most common land-surface parameters (slope, aspect, upslope area, topographic index). They

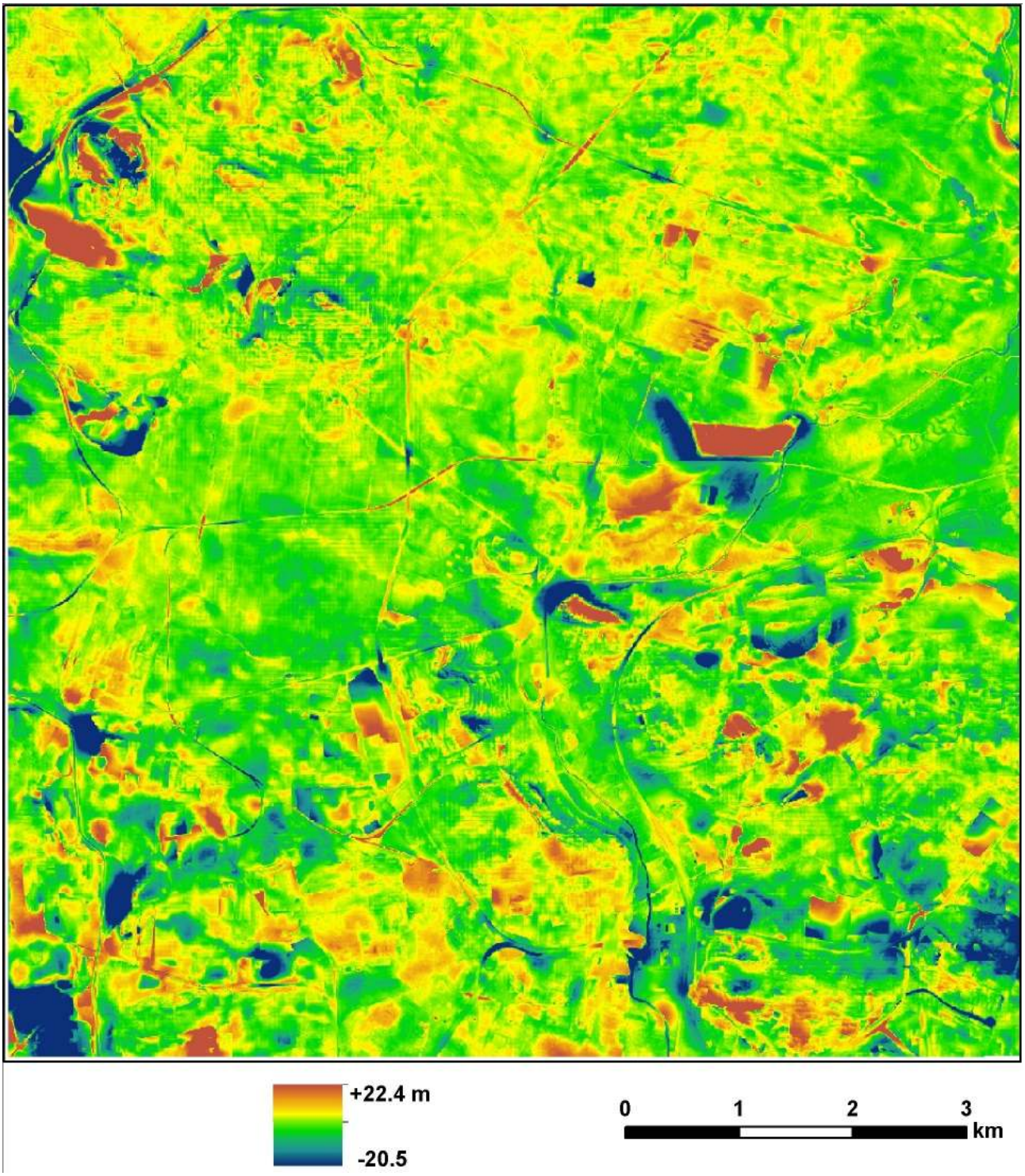

Figure 8: Spatial distribution of elevational changes between LiDAR-DEM and Topo-DEM

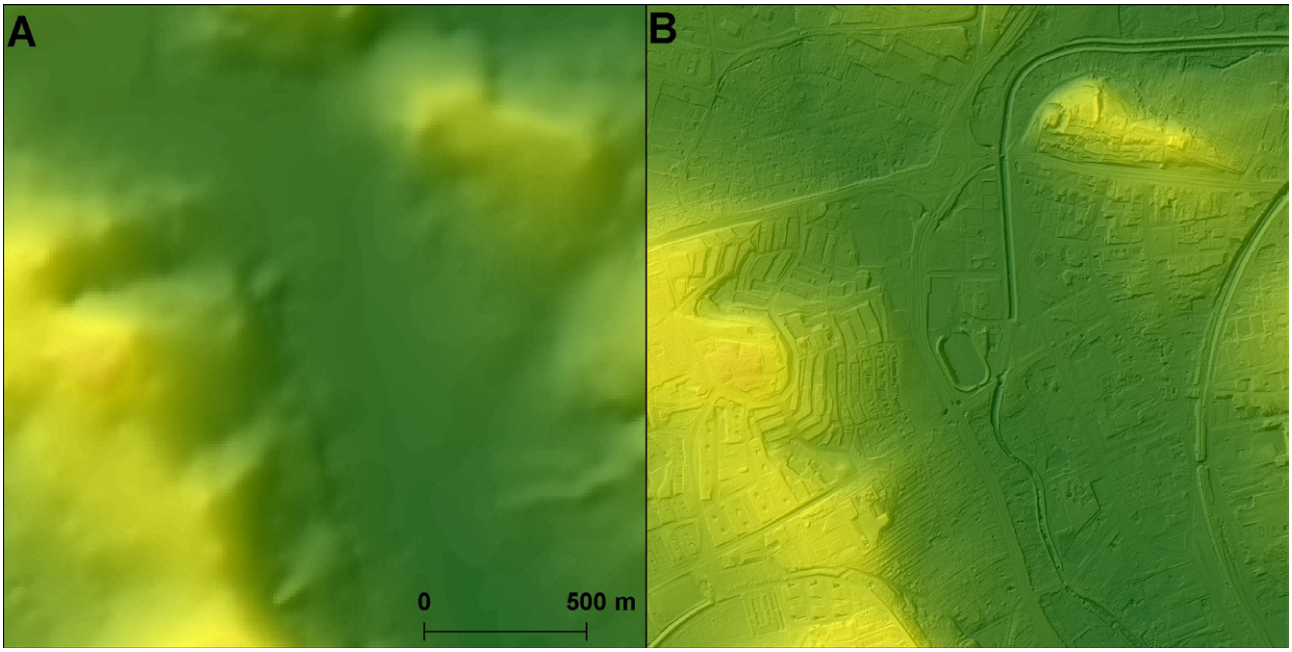

Figure 9: Details of hypsometry of the Topo-DEM (A) and LiDAR-DEM (B)

concluded that systematic errors can be reduced if a higher number of neighbours is used to derive local land-surface parameters (*e.g.* slope).

Another parameter is slope, which is the maximum rate of change in value from that cell to its neighbors. Basically, the maximum change in elevation over the distance between the cell and its eight neighbors (3×3) identifies the steepest downhill descent from the cell, expressed in degrees [71]. The spatial image of the calculated slopes is very similar to the local relief in the 3×3 cells neighborhood. Certainly, LiDAR-DEM showed a lot of small forms (lines of embankments and road incisions) that cannot be seen on Topo-DEM. However, the main features of the relief are very clear: St. Dorothy Hill in the NW, the wide valley of the Czarna Przemsza river in the central part and rows of ridges on its both sides in the south of the area (see Figure 1 and Figure 10). Higher maximum slope values occur in LiDAR-DEM but the mean and SD values are more similar (Table 3).

Curvature parameter describes the shape of a slope. This tool calculates the second derivative value of the input surface on a cell-by-cell basis. For each cell, a fourth-order polynomial of the form is fit to a surface composed of a 3×3 cells window [71]. One used standard curvature, which combines both the profile and plan curvatures (the units are 1/100 of meters). Usually, expected values for a hilly area (moderate relief) can vary from −0.5 to +0.5, while for steep and mountainous relief the values can be much higher. In this case, a picture of spatial distribution is much more interesting than the values themselves (Figure 11). The curvature map on the basis of Topo-DEM (Figure 11A) is clear and reflects and highlights characteristic elements of the topography well. Unfortunately, the map based on LiDAR-DEM (Figure 11B) is practically unreadable due to being too detailed, even though both maps are in the same resolution (10×10 m).

The last analyzed parameter was aspect. Aspect (slope direction) identifies the downslope direction of the maximum rate of change in value from each cell to its neighbors; values indicate the compass direction measured clockwise, expressed in degrees. A moving 3x3 cell window visits each cell in the input raster, and for each cell in the center of the window, an aspect value is calculated using an algorithm that incorporates the values of the cell's eight neighbors [71]. The Figure 12, with the distribution of the aspects, shows that a map derived from Topo-DEM is much better for analyzing because the image is more generalized (Figure 12A). LiDAR-DEM aspects introduce too much noise, so the picture is not clear (Figure 12B). The analysis of the polar plot and the percentage values for particular directions (Table 3) clearly show that the general quantitative-statistical picture is the same for both DEMs. The differences in percentage values between DEMs aspects are very small and range from 0.3 to 1.7%, mean 0.7%.

Generally, one has to state that Topo-DEM deals with this variable very well; this DEM clearly shows the course

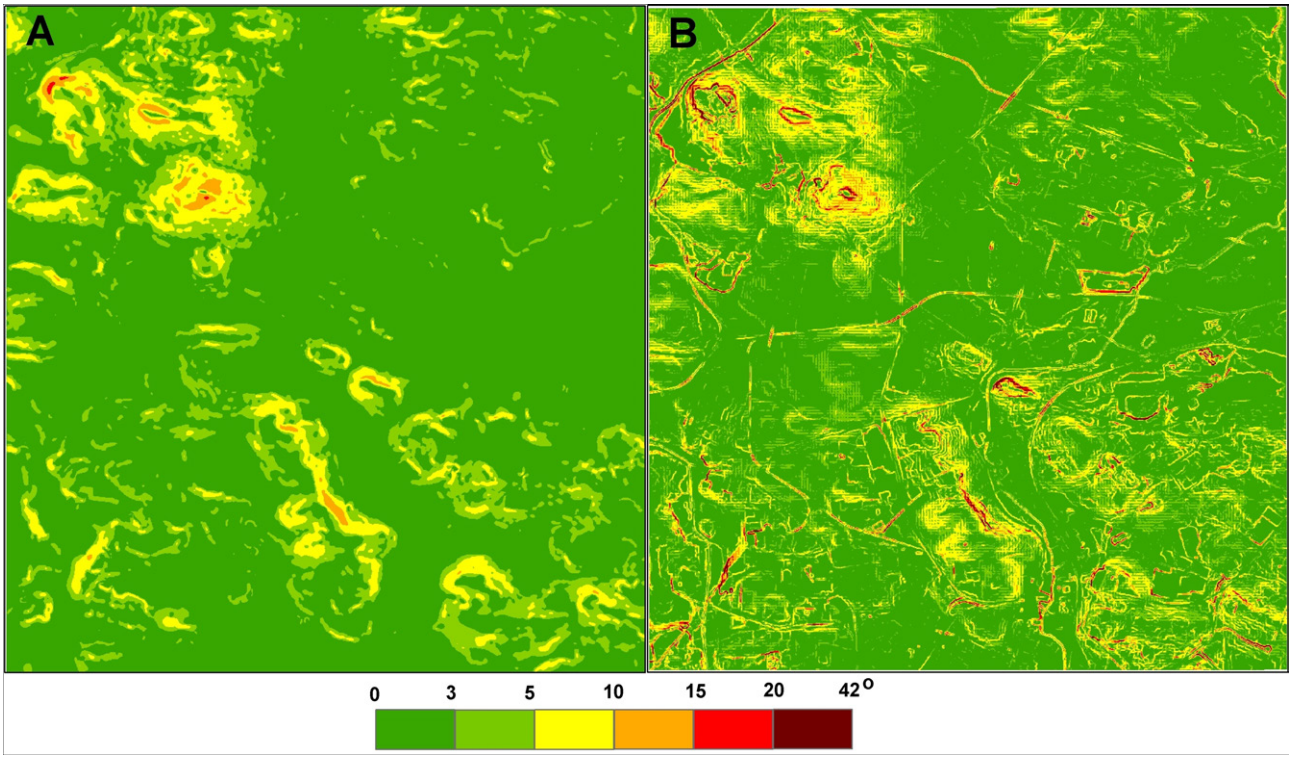

Figure 10: Slope map derived from Topo-DEM (A) and LiDAR-DEM (B)

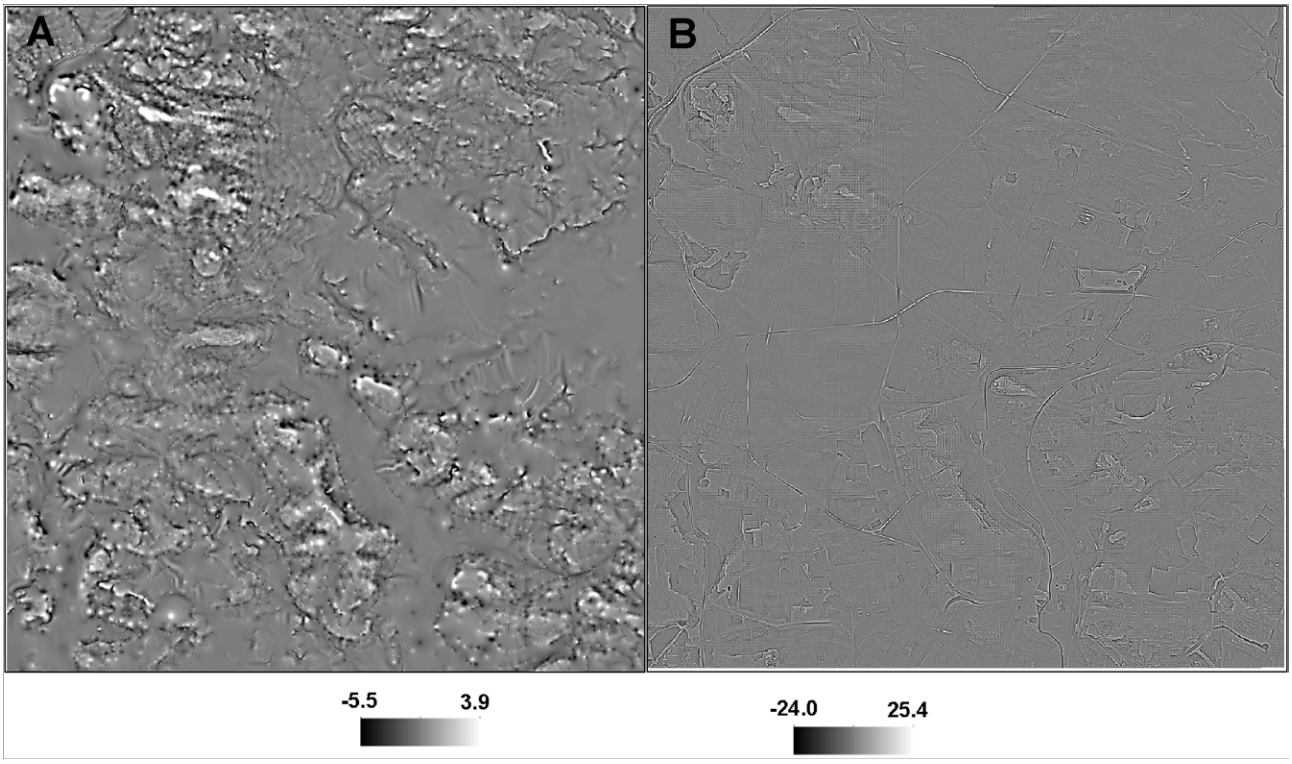

Figure 11: Curvature map derived from the Topo-DEM (A) and LiDAR-DEM (B)

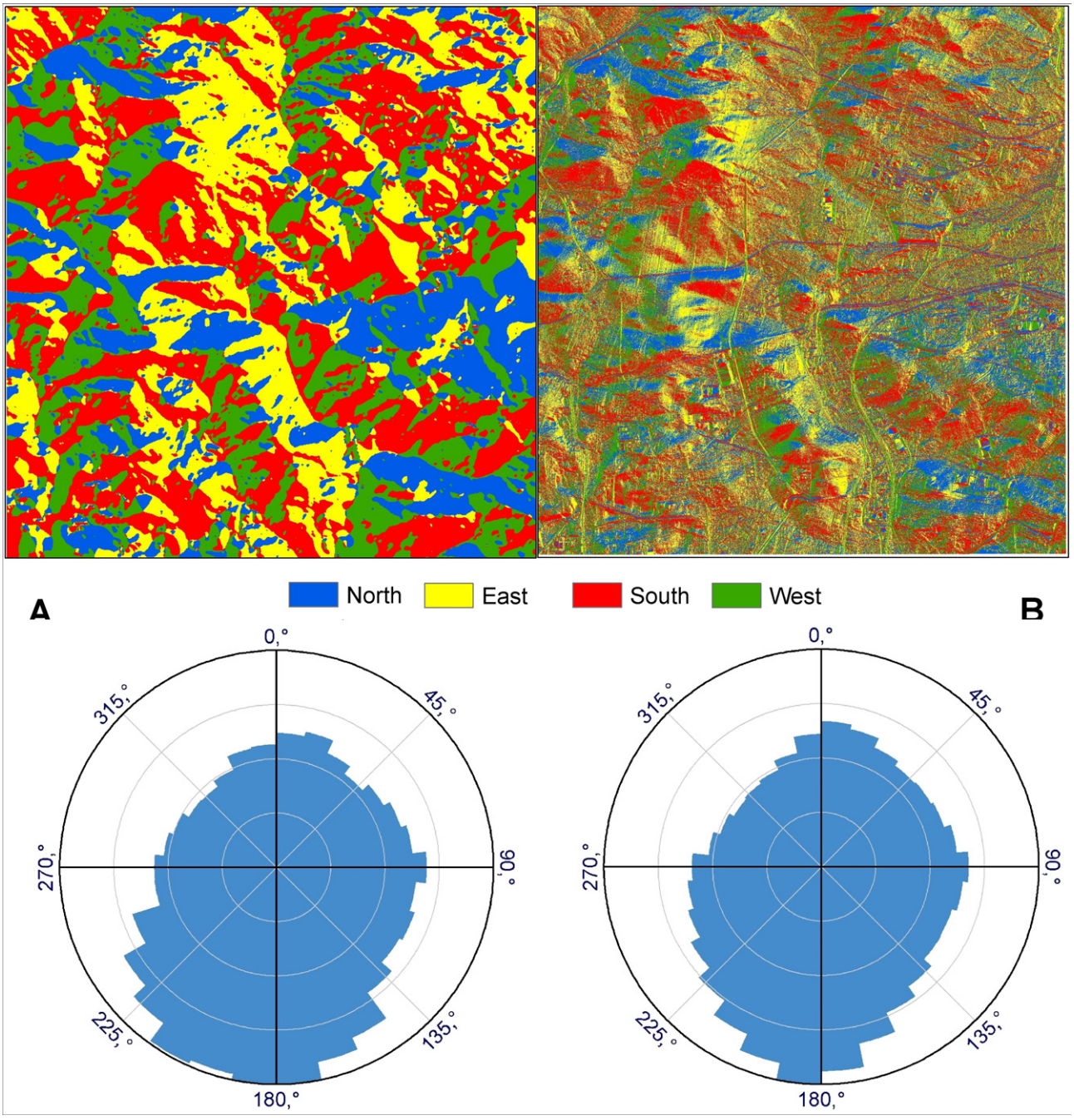

Figure 12: Spatial distribution and aspect map derived from Topo-DEM (A) and LiDAR-DEM (B)

of the main ridge-lines and river valleys, as well as large areas of slopes with a specific aspect.

5.3.3 Landform classification

It was decided to use Topographic Position Index (TPI) method to landform classification. Landform category can be determined by classifying the landscape using 2 TPI grids at different scales (large and small). Combining TPI at a small and large scale allows one to distinguish a variety of nested landforms. The general rule is that the range of TPI values increases with scale because elevation tends to be spatially autocorrelated [84]. After various experiments, It was decided to apply 10-class landform classification proposed by Weiss [84] using extension for ArcGIS [92]. The best results were achieved with the settings: small neighbourhood = 50 cells, and large = 350 cells (Fig-

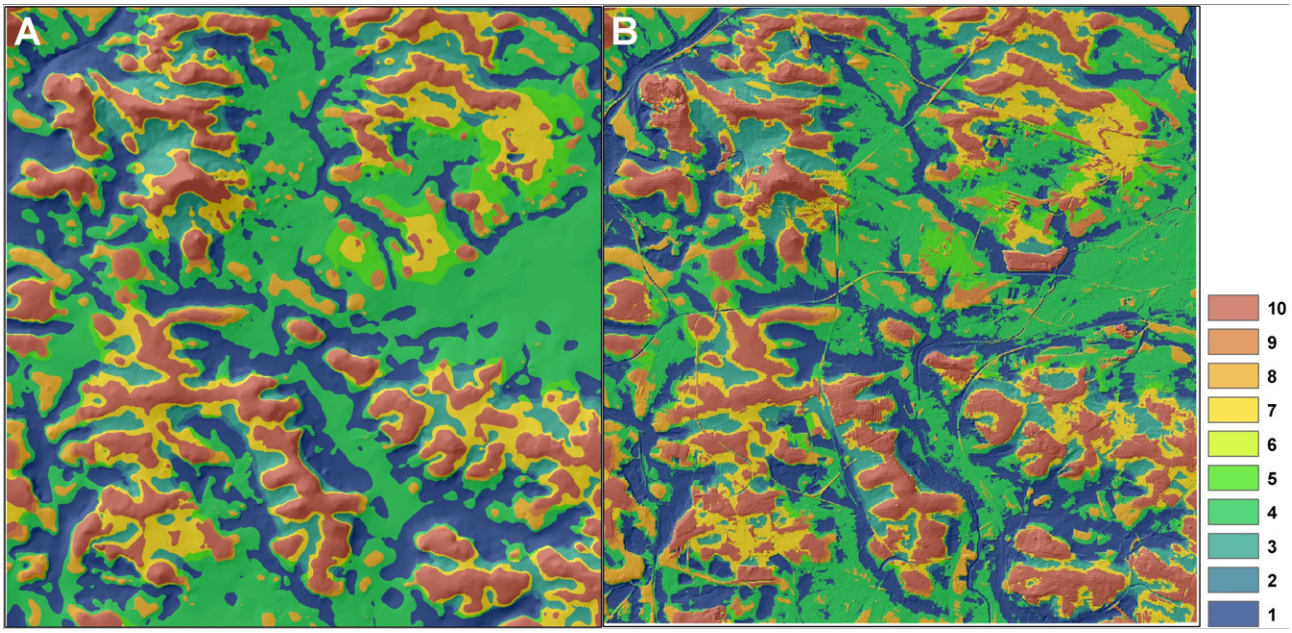

Figure 13: Landform classification into 10 classes with TPI method on the base Topo-DEM (A) and LiDAR-DEM (B) (number class explanations in Table 8)

Table 8: Landform classes on the base TPI method (after Weiss [78] slightly modified)

Class No.	Landform classes	Area of the landforms [%]	
		Topo-DEM	LiDAR-DEM
1	canyons, deeply incised streams	21.9	22.9
2	midslope drainages, shallow valleys	1.7	1.9
3	upland drainages, headwaters	7.7	8.0
4	u-shaped valleys, wide valleys and depressions	29.5	26.5
5	plains small	4.2	3.7
6	open slopes	0.1	0.3
7	upper slopes, mesas	11.2	10.5
8	local ridges, hills in valleys	4.6	6.0
9	midslope ridges, small hills in plains	1.8	2.1
10	mountain tops, high ridges	17.4	18.2
	Total:	**100.0**	**100.0**

ure 13). In general, spatial distribution of the main landforms is similar. Classification on the basis of of the Topo-DEM is more balanced, slightly generalized compared to LiDAR-DEM. It seems that better visual effects are given by Topo-DEM classification; the image is less overloaded. Although the reality is probably more efficiently reflected by LiDAR-DEM, the reception of the simplified (generalized) image is much better and easier to understand because we focus on dominant elements, avoiding unnecessary details. Moreover, quantitative analysis of landforms (Table 8) showed that results from both models were almost identical (the same statistical image). The maximum percentage differences between DEMs are small and range from 0.2 to 3.0%. As part of the experiment a median filter (window 10×10 cell) was applied to classify LiDAR-DEM classification. The obtained spatial image was very similar to the Topo-DEM results and the compared percentages showed differences ranging from 0.1 to 1.2%. One can conclude that Topo-DEM is a very good simplification (generalization) of LiDAR-DEM for landform classification analysis. Some studies have shown that LiDAR-DEMs need to be resampled to coarser resolution to be more useful for the

extraction of scale-appropriate hydrographic and other geomorphic features [93–95].

6 Conclusions

The conclusions arising from this paper are as follows:

1. Elevation accuracy of the analyzed Topo-DEM in 10×10 m resolution corresponds to the precision of the source topographic maps (1:10,000) with the mean error of 1-2 m. These results have been confirmed by GPS RTK measurements (MAE was 0.72 m and RMSE/SD <1 m) and compared with the LiDAR-DEM (MAE 1.16 m, RMSE 1.69 m and SD 1.83 m).
2. Among the compared models (except for Topo-DEM), the DTED-2 model achieved the best results. Maximum altitude errors did not exceed 6 m, while the MAE was 1.3 m, and RMSE was 1.7 m. For a DEM with a resolution of about 25×25 m these are surprisingly good results, especially if we remember that the DTED-2 was made from the digitalization of the military topographic maps 1:50,000.
3. LiDAR-DEM with 1x1 m resolution, and even converted to a 10×10 m (downsampling), is great DEM, but it turned out to be too detailed for an area of this size (tens of km^2). This had a particularly adverse effect on maps with geomorphometric parameters (slope, curvatures, aspects) and landform classifications. Too much detail caused information overload and blurred the spatial image, making maps unreadable.
4. A Topo-DEM model coped well with the presentation of topography: it emphasized and reflected the most characteristic and dominant relief features. Maps of derived geomorphometric parameters and landform classification showed statistical and spatial distribution of the relief very well. These results confirmed the significance of geomorphological accuracy in geomorphometric analysis, where correct reflection of the character and leading morphology features more important than absolute height accuracy of a DEM and its detailed conformity with reality.
5. The above informations about Topo-DEMs may be useful when:
   - there is no high-resolution DEM derived from LiDAR for the given area, but there are topographic maps that can be used to create a Topo-DEM; such Topo-DEM will be reliable and accurate;
   - there is a need to create a DEM of a given area based on historic topographic maps and compare it with the contemporary DEM (*i.e.* LiDAR), it is important for studies of the areas heavily transformed by man;
   - Topo-DEM can be used as reliable data to reduce the errors of freely-available global DEMs (*e.g.* for some areas in Poland SRTM has a plenty of errors).

Acknowledgement: I wish to thank to Instrumenty Geodezyjne T. Nadowski company for access to GNSS corrections during the GPS RTK surveys.

References

[1] Migoń P., Kasprzak M., Traczyk A., How high-resolution DEM based on airborne LiDAR helped to reinterpret landforms – examples from the Sudetes, SW Poland. Landform Analysis, 2013, 22, 89–101. DOI: 10.12657/landfana.022.007

[2] Wieczorek M., Migoń P., Automatic relief classification versus expert and field based classification for the medium-altitude mountain range, the Sudetes, SW Poland. Geomorphology, 2014, 206, 133–146. DOI: 10.1016/j.geomorph.2013.10.005

[3] Iwahashi J., Pike R.J., Automated classification of topography from DEMs by an unsupervised nested-mean algorithm and a three-part geometric signature. Geomorphology, 2007, 86, 409–440. DOI: 10.1016/j.geomorph.2006.09.012

[4] Drăguţ L., Eisank C., Object representations at multiple scales from digital elevation models. Geomorphology, 2011, 129, 183-189. DOI: 10.1016/j.geomorph.2011.03.003

[5] Drăguţ L., Eisank C., Automated object-based classification of topography from SRTM data. Geomorphology, 2012, 141–142, 21-33. DOI: 10.1016/j.geomorph.2011.12.001.

[6] Piloyan A., Konečný M., Semi-automated classification of landform elements in Armenia based on SRTM DEM using *k*-means unsupervised classification. Quaestiones Geographicae, 2017, 36(1), 93-103. DOI: 10.1515/quageo-2017-0007

[7] Gallant J.C, Dowling T.I., A multiresolution index of valley bottom flatness for mapping depositional areas. Water Resources Research, 2003, 39(12), 1347. DOI: 10.1029/2002WR001426

[8] Jasiewicz J., Stepinski T.F., Geomorphons - a pattern recognition approach to classification and mapping of lanforms. Geomorphology, 2013, 182, 147-156. DOI: 10.1016/j.geomorph.2012.11.005.

[9] Szypuła B., Quantitative studies of the morphology of the south Poland using Relief Index (RI). Open Geosciences, 2017, 9, 509-524. DOI: 10.1515/geo-2017-0039

[10] Moudrý V., Lecours V., Gdulová K., Gabor L., Moudrá L., Kropáček J., Wild J., On the use of global DEMs in ecological modelling and the accuracy of new bare-earth DEMs. Ecological Modelling, 2018, 383. DOI: 10.1016/j.ecolmodel.2018.05.006.

[11] Shearer J.W., The accuracy of digital terrain models. In: Petrie G., Kennie T.J.M. (eds), Terrain Modeling in Surveying and Engineering. Whittles Publishing Services: Caithness, 1990, 315–336.

[12] Desmet P.J.J., Effects of interpolation errors on the analysis of DEMs. Earth Surface Processes and Landforms, 1997, 22, 563–580. DOI: 10.1002/(SICI)1096-9837(199706)22:6<563::AID-ESP713>3.0.CO;2-3.
[13] Florinsky I.V., Accuracy of local topographic variables derived from digital elevation models. International Journal of Geographical Information Science, 1998, 12, 47-61.
[14] Chaplot V., Darboux F., Bourennane H., Leguédois S., Silvera N., Phachomphon K., Accuracy of interpolation techniques for the derivation of digital elevation models in relation to landform types and data density. Geomorphology, 2006, 77, 126–141. DOI: 10.1016/j.geomorph.2005.12.010
[15] Reuter H.I., Hengl T., Gessler P., Soille P., Preparation of DEMs for Geomorphometric Analysis. In: Hengl T., Reuter H.I. (eds), Geomorphometry: Concepts, Software, Applications. Developments in Soil Science 33, Elsevier, Amsterdam, 2009, 87–120. DOI: 10.1016/S0166-2481(08)00004-4
[16] Fisher P.F., Tate N.J., Causes and consequences of error in digital elevation models. Progress in Physical Geography, 2006, 30, 467-489. DOI:10.1191/0309133306pp492ra
[17] Wise S.M., The effect of GIS interpolation errors on the use of DEMs in geomorphology. In: Lane S.N., Richards K.S., Chandler J.H. (eds), Landform Monitoring, Modeling and Analysis. Wiley, Chichester, 1998, 139–164.
[18] Florinsky I.V., Errors of signal processing in digital terrain modelling. International Journal of Geographical Information Science, 2002, 16(5), 475–501. DOI: 10.1080/13658810210129139
[19] Thomas J., Prasannakumar V., Vineetha P., Suitability of spaceborne digital elevation models of different scales in topographic analysis: an example from Kerala, India. Environmental Earth Sciences, 2015, 73(3), 1245-1263. DOI: 10.1007/s12665-014-3478-0
[20] Zhang W., Montgomery D., Digital elevation model grid size, landscape representation, and hydrologic simulations. Water Resources Research, 1994, 30(4), 1019–1028.
[21] Li Z.L., A comparative study of the accuracy of digital terrain models (DTMs) based on various data models. ISPRS Journal of Photogrammetry and Remote Sensing, 1994, 49, 2-11.
[22] Aguilar F.J., Agüera F., Aguilar M.A., Carvajal F., Effects of terrain morphology, sampling density, and interpolation methods on grid DEM accuracy. Photogrammetric Engineering and Remote Sensing, 2005, 71, 805-816. DOI: 10.14358/PERS.71.7.805
[23] Bolstad P.V., Stowe T., An evaluation of DEM accuracy: Elevation, slope, and aspect. Photogrammetric Engineering and Remote Sensing, 1994, 60, 1327-1332.
[24] Edson C., Wing M.G., LiDAR Elevation and DEM Errors in Forested Settings. Modern Applied Science, 2015, 9(2), 139-157. DOI: 10.5539/mas.v9n2p139.
[25] Contreras M.A., Staats W., Yiang J., Parrott, D., Quantifying the Accuracy of LiDAR-Derived DEM in Deciduous Eastern Forests of the Cumberland Plateau. Journal of Geographic Information System, 2017, 9, 339-353. DOI: 10.4236/jgis.2017.93021
[26] Karamouz M., Fereshtehpour M., Modeling DEM Errors in Coastal Flood Inundation and Damages: A Spatial Non-stationary Approach. Water Resources Research, 2019, 1-19. DOI: 10.1029/2018WR024562.
[27] Yamazaki D., Ikeshima D., Tawatari R., Yamaguchi T., O'Loughlin F., Neal J.C., Sampson C.C., Kanae S., Bates P.D., A high-accuracy map of global terrain elevations: Accurate Global Terrain Elevation map. Geophysical Research Letters, 2017, 44(11), 5844–5853. DOI: 10.1002/2017GL072874
[28] McMaster K.J., Effects of digital elevation model resolution on derived stream network positions. Water Resources Research, 2002, 38(4), 13-1 -13-8. DOI: 10.1029/2000WR000150
[29] Persendt F.C., Gomez C., Assessment of drainage network extractions in a lowrelief area of the Cuvelai Basin (Namibia) from multiple sources: LiDAR, topographic maps, and digital aerial orthophotographs. Geomorphology, 2016, 260, 32–50. DOI: 10.1016/j.geomorph.2015.06.047
[30] Das S., Patel P.P., Sengupta S., Evaluation of Different Digital Elevation Models for Analyzing Drainage Morphometric Parameters in a Mountainous Terrain: A Case Study of the Supin-Upper Tons Basin, Indian Himalayas. SpringerPlus, 2016, 5, 1544. DOI: 10.1186/s40064-016-3207-0
[31] Purinton B., Bookhagen B., Validation of digital elevation models (DEMs) and comparison of geomorphic metrics on the southern central Andean plateau. Earth Surface Dynamics, 2017, 5(2), 211–237. DOI: 10.5194/esurf-5-211-2017
[32] Boulton S.J., Stokes M., Which DEM is best for analyzing fluvial landscape development in mountainous terrains? Geomorphology, 2018, 310, 168–187. DOI: 10.1016/j.geomorph.2018.03.002
[33] Hutchinson M.F., Stein J.A., Stein J.L., Xu T., Locally adaptive gridding of noisy high resolution topographic data. In: 18th World IMACS / MODSIM Congress, Cairns, Australia 13-17 July 2009, 2493-2499.
[34] Pike R.J., Evans I.S., Hengl T., Geomorphometry: A Birief Guide. In: Hengl T., Reuter H.I. (Eds.), Geomorphometry. Concepts, Software, Applications. Elsevier, 2009, 3-30. DOI: 10.1016/S0166-2481(08)00001-9.
[35] Kondracki J., Geografia regionalna Polski (Regional geography of Poland). PWN, Warszawa, 2001, 441 p. (in Polish)
[36] Biernat S., sheet M-34-51-C Wojkowice. Detailed Geological Map of Poland (1:50 000). Geological Institute, 1955.
[37] Biernat S., Krysowska M., sheet M-34-63-A Katowice. Detailed Geological Map of Poland (1:50 000). Geological Institute, 1956.
[38] Jania J., Dulias R., Szypuła B., Tyc A., Digital Geomorphological Map of Poland 1:100,000, sheet Katowice. Warszawa. Surveyor General of Poland, 2014.
[39] LiDAR-DEM (ESRI ASCII Grid). Surveyor General of Poland, Warszawa, 2014.
[40] CODGiK (Central Office of Geodesy and Cartography), Digital elevation data, 2015. http://www.codgik.gov.pl/index.php/zasob/numeryczne-dane-wysokosciowe.html
[41] Szypuła B., Geomorphometric comparison of DEMs built by different interpolation methods. Landform Analysis, 2016, 32, 45-58. DOI: 10.12657/landfana.032.004
[42] DTED-2 (Digital Terrain Elevation Data of Poland, level 2), Military Geodesy and Remote Sensing Centre, Warszawa, 2001.
[43] Czajka W., Baza danych wysokości terenu w formacie DTED (Database of the terrain elevations in DTED format). BELLONA (special issue). MON, Warszawa, 2009, 26-30 (in Polish).
[44] DMA (Defense Mapping Agency), Performance Specification Digital Terrain Elevation Data (DTED), MIL-PRF-89020B, 2000, 45 p.
[45] SRTM v3 (NASA Shuttle Radar Topography Mission Global 1 arc second V003). NASA Jet Propulsion Laboratory, 2013.
[46] Farr T.G., Rosen P.A., Caro E., Crippen R., Duren R., Hensley S., Kobrick M., Paller M., Rodriguez E., Roth L., Seal D., Shaffer S., Shimada J., Umland J., Werner M., Oskin M., Burbank D., Alsdorf D., The Shuttle Radar Topography Mission. Reviews of Geophysics,

200, 45(2), 1-43. DOI: 10.1029/2005RG000183
[47] Rodriguez E., Morris C.S., Belz J., Chapin E., Martin J., Daffer W., Hensley S., An Assessment of the SRTM Topographic Products, Technical Report JPL D-31639, Jet Propulsion Laboratory, Pasadena, California, 2005, 143 p.
[48] Rodriguez E., Morris C.S., Belz J.E., A global assessment of the SRTM performance, Photogramm. Eng. Remote Sens., 2006, 72, 249–260. DOI: 10.14358/PERS.72.3.249
[49] Tachikawa T., Kaku M., Iwasaki A., ASTER GDEM Version 2 Validation Report. Report to the ASTER GDEM Version 2 Validation Team, 2011.
[50] Danielson J.J., Gesch D.B., Global multi-resolution terrain elevation data 2010 (GMTED2010). U.S. Geological Survey Open-File Report 2011–1073, 2011, 26 p.
[51] Kobrick M., Crippen R., SRTMGL1N: NASA Shuttle Radar Topography Mission Global 1 arc second number V003, 2014. DOI: 10.5067/MEaSUREs/SRTM/SRTMGL1N.003
[52] ASTER GDEM (ASTER Global Digital Elevation Model). NASA and METI, U.S./Japan ASTER Science Team, 2009.
[53] ASTER GDEM Validation Team, ASTER Global DEM Validation Summary Report. 2009, 28 p.
[54] Tachikawa T., Hato M., Kaku M., Iwasaki A., The characteristics of ASTER GDEM version 2. IEEE International Geoscience and Remote Sensing Symposium, IGARSS 2011, Vancouver, BC, Canada, July 24-29, 2011. DOI: 10.1109/IGARSS.2011.6050017
[55] AW3D30 v1.1 (ALOS Global Digital Surface Model "ALOS World 3D - 30m). Earth Observation Research Center (EORC), Japan Aerospace Exploration Agency (JAXA), 2017.
[56] Tadono T., Ishida H., Oda F., Naito S., Minakawa K., Iwamoto H., Precise global DEM generation by ALOS PRISM. ISPRS Annals of the Photogrammetry, Remote Sensing and Spatial Information Sciences, 2014, II-4, 71-76. DOI: 10.5194/isprsannals-II-4-71-2014
[57] Takaku J., Tadono T., Tsutsui K., Generation of high resolution Global DSM from ALOS PRISM. The International Archives of the Photogrammetry, Remote Sensing and Spatial Information Sciences XL-4, ISPRS TC IV Symposium, Suzhou, China, 2014, pp 243-248. DOI: 10.5194/isprsarchives-XL-4-243-2014
[58] EORC (Earth Observation Research Center) and JAXA (Japan Aerospace Exploration Agency), ALOS Global Digital Surface Model (DSM) “ALOS World 3D-30m” (AW3D30) Dataset Product Format Description version 1.1. 2017, 8 p. http://www.eorc.jaxa.jp/ALOS/en/aw3d30.html
[59] EU-DEM v1.1 (European Digital Elevation Model, version 1.1). European Environment Agency (EEA) under the framework of the Copernicus programme, 2016.
[60] Dufourmont H., Gallego J., Reuter H., Strobl P., EU-DEM Statistical Validation Report. 2014, 27 p.
[61] EU-DEM Metadata, 2016. http://www.eea.europa.eu/data-and-maps/data/eu-dem#tab-metadata.html
[62] Topographic Map of Poland, 1:10,000 sheets: M-34-51-C-c-4, M-34-51-C-d-3, M-34-63-A-a-2, M-34-63-A-b-1. Head Office of Geodesy and Cartography, Warszawa, 1993
[63] Kimerling A.J., Mathematical relationships among map scale, raster data resolution, and map display resolution. https://blogs.esri.com/esri/arcgis/2009/12/04/mathematical-relationships-among-map-scale-raster-data-resolution-and-map-display-resolution Accessed 26 June 2018
[64] Kadaj R.J., Polskie układy współrzędnych. Formuły transformacyjne, algorytmy i programy. AlgoRes soft, Rzeszów, 2002, 52 p (in Polish).
[65] ESRI (Environmental Systems Research Institute), ArcGIS Desktop: Release 10.5. Redlands, CA, 2017.
[66] Hutchinson M.F., Calculation of hydrologically sound digital elevation models. Paper presented at Third International Symposium on Spatial Data Handling at Sydney, Australia, 1988.
[67] Hutchinson M.F., A new procedure for gridding elevation and stream line data with automatic removal of spurious pits. Journal of Hydrology, 1989, 106, 211–232.
[68] Hutchinson M.F., A locally adaptive approach to the interpolation of digital elevation models. In: Proceedings, Third International Conference/Workshop on Integrating GIS and Environmental Modeling. Santa Barbara, CA: National Center for Geographic Information and Analysis, 1996.
[69] Hutchinson M.F., Adding the Z-Dimension. In: Handbook of Geographic Information Science, Blackwell, 2008.
[70] Hutchinson M.F., ANUDEM Version 5.3. User Guide. Fenner School of Environment and Society, Australian National University. 2011, 25 p.
[71] ArcGIS Help 10.5 http://desktop.arcgis.com/en/arcmap/latest.html
[72] Höhle J., Höhle M., Accuracy assessment of digital elevation models by means of robust statistical methods. ISPRS Journal of Photogrammetry and Remote Sensing, 2009, 64(4), 398-406. DOI: 10.1016/j.isprsjprs.2009.02.003
[73] Maune D.F., (ed.) Digital Elevation Model Technologies and Applications: The DEM User Manual, 2nd ed. American Society for Photogrammetry and Remote Sensing, 200, 656 p.
[74] Flood M., (ed) ASPRS Guidelines Vertical Accuracy Reporting for Lidar Data v.1.0. ASPRS Lidar Committee (PAD), 2004, 20 p.
[75] Rieger W., Accuracy of slope information derived from DEM-data. International Archives of Photogrammetry and Remote Sensing, 1996, 31(B4), 690-695.
[76] Fisher P.F., Improved modeling of elevation error with geostatistics. GeoInformatica, 1998, 2(3), 215–233.
[77] Schneider B., Geomorphologically plausible reconstruction of the digital representation of terrain surfaces from contour data. Ph.D. Thesis. Universtiy of Zürich, 1998 (in German)
[78] Wise S.M., Assessing the quality for hydrological applications of digital elevation models derived from contours. Hydrological Processes, 2000, 14(11–12), 1909–1929. DOI: 10.1002/1099-1085(20000815/30)14:11/12<1909::AID-HYP45>3.0.CO;2-6
[79] Szypuła B., Digital elevation models in geomorphology. In: Shukla D.P. (ed.) Hydro-Geomorphology - Models and Trends. InTechOpen, 2017b, 81-112. DOI: 10.5772/intechopen.68447
[80] Evans I.S., General geomorphometry, derivatives of altitude, and descriptive statistics. In: Chorley R.J. (ed.) Spatial Analysis in Geomorphology. Harper & Row, New York, 1972, 17-90.
[81] Krcho J., Morphometric analysis of relief on the basis of geometric aspect of field theory. Acta geographica Universitatis Comenianae, Geographico-physica, 1973, 1, 11-233.
[82] Szypuła B., Wieczorek M., Geomorfometryczna analiza rzeźby Wyżyny Śląskiej metodą wskaźnika TPI (Geomorphometric analysis of relief of the Silesian Upland by the TPI method). In: Żyszkowska W., Spallek W. (eds.) Główne problemy współczesnej kartografii. Zastosowanie statystyki w GIS i kartografii. Wrocław, 2011, 73–82 (in Polish with English summary)
[83] Fels J.E., Zobel R., Landscape position and classified landtype mapping for statewide DRASTIC mapping project. North Carolina State University technical report VEL.95.1, 1995.

[84] Weiss A., Topographic positions and landforms analysis (Conference Poster). ESRI International User Conference. San Diego, CA, 2001, 9-13.
[85] Li Z.L., On the measure of digital terrain model accuracy. Photogrammetric Record, 1988, 12(72), 873–877.
[86] Ghahramani S., Fundamentals of Probability (2nd Edition). Prentice Hall, New Jersey, 2000, 438 p.
[87] Borkowski A., Numeryczne modele wysokościowe i produkty pochodne. In: Wężyk P., (ed.) Podręcznik dla uczestników szkoleń z wykorzystania produktów LiDAR. GUGiK, Warszawa, 2014, pp 110-131 (in Polish)
[88] Büyüksalih G., Kocak G., Oruc M., Akcin H., Jacobsen K., Accuracy Analysis, DEM Generation and Validation using Russian TK-350 Stereo-Images. The Photogrammetric Record, 2004, 19(107), 200-218.
[89] Li Z.L., Variation of the accuracy of digital terrain models with sampling interval. Photogrammetric Record, 1992, 14, 113–128.
[90] Sharma A., Tiwari K.N., Bhadoria P.B.S., Measuring the Accuracy of Contour Interpolated Digital Elevation Models. Journal of Indian Society of Remote Sensing, 2009, 37, 139–146. DOI: 10.1007/s12524-009-0005-y
[91] Raaflaub L.D., Collins M.J., The effect of error in gridded digital elevation models on the estimation of topographic parameters. Environmental Modelling & Software, 2006, 21, 710–732. DOI: 10.1016/j.envsoft.2005.02.003
[92] Jenness J., Brost B., Beier P., Land Facet Corridor Designer: Extension for ArcGIS. Jenness Enterprises, 2013 http://www.jennessent.com/arcgis/land_facets.html
[93] Chen J., Lin G., Yang Z., Chen H., The relationship between DEM resolution, accumulation area threshold and drainage network indices. 18th International Conference on Geoinformatics, 2010, 1–5.
[94] Dougherty M., Assessment of Digital Elevation Model Accuracy on the St. John's New Madrid Shorebird Habitat Model. U.S. Army Corps of Engineers Memphis District. 2011, 10 p.
[95] Metz M., Mitasova H., Harmon R.S., Efficient extraction of drainage networks from massive, radar-based elevation models with least cost path search. Hydrology and Earth System Sciences, 2011, 15(2), 667–678. DOI: 10.5194/hess-15-667-2011